

Heavy flavor hadrons from multi-body Dirac equations

Shuzhe Shi^{a,b}, Jiaxing Zhao^{a,b}, and Pengfei Zhuang^a

^a*Physics Department, Tsinghua University, Beijing 100084, China*

^b*Department of Physics, McGill University, Montreal, QC H3A 2T8, Canada*

(Dated: December 27, 2022)

We systematically solve the two- and three-body Dirac equations for heavy flavor hadrons. By spherical harmonic oscillator expansion of the baryon wave function, we calculate the baryon mass, mean radius, total angular momentum and parity for ground and excited states. With a universal set of quark mass and coupling parameters for both mesons and baryons, the calculated hadron masses agree well with the experimental data, with relative difference $< 2.5\%$ for mesons and $< 6.3\%$ for baryons.

I. INTRODUCTION

Considering the big difference between heavy and light quark masses, heavy flavor hadrons, including open and closed heavy flavors, play a significant role in understanding the properties of quantum chromodynamics (QCD) in vacuum and hot medium. Recently, many experimental efforts as well as achievements have been made in searching for multi-charmed baryons to complete and verify the particle zoo predicted by the flavor $SU(4)$ quark model, for instance, the discovery of doubly charmed baryon Ξ_{cc}^{++} [1] and charmonium-pentaquark state ($c\bar{c}uud$) [2]. Theoretically, hadron properties are widely studied in effective models at quark level, such as lattice QCD [3–7], QCD sum rules [8], Bethe–Salpeter equation [9], and chiral quark models [10].

For hadrons including only heavy quarks, such as J/ψ , B_c , Υ and Ω_{ccc} , one can safely neglect the heavy quark creation-annihilation fluctuations and study their static properties in vacuum and at finite temperature in non-relativistic potential models [11, 12]. The potential models are also extended to study open heavy flavor states like D mesons and Ξ_{cc} baryons [13–16]. For heavy flavor hadrons with a typical radius ~ 0.5 fm, the uncertainty principle leads to a characteristic momentum around ~ 0.4 GeV, corresponding to a relative velocity $v \sim c$ between the two constituents of a D meson. Therefore, the relativistic effect should seriously be taken into account, especially for the open heavy flavor states. On the other hand, the spin interaction, which results in the fine structure of hadron mass spectra [16] and becomes more important in multi-quark states, is a relativistic effect and should self-consistently be introduced in the covariant Dirac equation.

The first completely covariant framework for a bound-state problem was presented in 1951 by Salpeter and Bethe [17] and Gell-Mann and Low [18] independently. In the original Bethe–Salpeter equation, the time dependence is entangled in a complicated way, and one is not able to find the stationary states. Along with many pioneer efforts [19, 20] to simplify the Bethe–Salpeter equation, the covariant wave equation proposed by Sazdjian [21] provides a way to find relativistic bound-state wave functions. In the meantime, Crater and Alstine developed the two-body Dirac equation [22–24] for mesons which covariantly converts the Dirac equation with 16 degrees of freedom into the Klein–Gordon-like equations with highly disentangled degrees of freedom. In this framework, one can clearly see the relativistic corrections to the non-relativistic potential, including the Darwin term and many spin interaction terms. Later on, the three-body Dirac equation for baryons was developed by Whitney and Crater [25], which combines Sazdjian’s N -body relativistic potential model with the two-body Dirac equation.

In this paper, we aim to systematically and precisely study the heavy flavor hadron spectra and wave functions. We adopt the two- and three-body Dirac equations for mesons and baryons, with the following improvements in solving the equations in comparison with the previous calculations:

- (i) For the three-body Dirac equation for baryons, we expand the baryon wave function in the Hilbert space constructed by spherical harmonic oscillators, which guarantees the completeness and orthogonality of the expansion, and therefore increases the accuracy of the calculation and can be used to systematically study the baryon ground and excited states.
- (ii) We take particle-index-rotation technique in calculating the Hamiltonian elements in the Hilbert space, which speeds up the calculation and improves further the precision of the calculation.
- (iii) We take a universal set of quark mass and coupling parameters for all the hadrons. This makes the calculation more self-consistent and predictable for future application of multi-body Dirac equations to the study of multi-quark bound states.

The paper is organized as follows. After a short introduction to the three-body Dirac equation for baryons, we present the improved way of numerically solving the equation in Section II. In Section III, we first discuss the convergency of the numerical calculation and then show the results on heavy flavor hadron masses and wave functions, with a universal set of parameters for both mesons and baryons. We summarize our study in Section IV. The details

on relativistic two-body potentials, spin and flavor states, particle-index-rotation technique, and Hamiltonian matrix elements are explicitly shown in Appendix A to D.

II. THREE-BODY DIRAC EQUATION

The two-body Dirac equation which is used to describe heavy flavor meson mass M_m and wave function $\Psi_m(\mathbf{r}_1, \mathbf{r}_2)$ is discussed in detail in Refs. [22–24] in vacuum and Refs. [26, 27] at finite temperature. We will focus in this section on the three-body Dirac equation for heavy flavor baryons. In the framework firstly developed by Whitney *et al* [25] based on Sazdjian's N -body relativistic potential model [21], the baryon wave function $\Psi_b(\mathbf{r}_1, \mathbf{r}_2, \mathbf{r}_3)$ is controlled by the Schrödinger-like equation,

$$\left[\sum_{i=1}^3 \frac{\mathbf{p}_i^2}{2\epsilon_i} + \sum_{i<j}^3 \frac{\epsilon_i + \epsilon_j}{2\epsilon_i \epsilon_j} \mathcal{V}_{ij} \right] \Psi_b = E \Psi_b, \quad (1)$$

where \mathbf{r}_i and \mathbf{p}_i are the quark coordinate and momentum, $E = 1/6 \sum_{ij} (\epsilon_i^2 - m_j^2)/\epsilon_i$ is the energy eigenvalue related to the effective quark mass ϵ_i and vacuum quark mass m_i , the baryon mass M_b is determined by the coupled equations,

$$\epsilon_i = \frac{M_b}{3} + \frac{1}{3} \sum_{j \neq i} \frac{m_i^2 - m_j^2}{\epsilon_i + \epsilon_j}, \quad (2)$$

and the interaction between two quarks is described by the relativistic potential $\mathcal{V}_{ij}(\mathbf{r}_{ij})$,

$$\begin{aligned} \mathcal{V}_{ij} = & 2m_{ij}S + S^2 + 2\epsilon_{ij}A - A^2 + \Phi_D + \boldsymbol{\sigma}_i \cdot \boldsymbol{\sigma}_j \Phi_{SS} + \mathbf{L}_{ij} \cdot (\boldsymbol{\sigma}_i + \boldsymbol{\sigma}_j) \Phi_{SO} + (\boldsymbol{\sigma}_i \cdot \hat{\mathbf{r}}_{ij})(\boldsymbol{\sigma}_j \cdot \hat{\mathbf{r}}_{ij}) \mathbf{L}_{ij} \cdot (\boldsymbol{\sigma}_i + \boldsymbol{\sigma}_j) \Phi_{SOT} \\ & + \mathbf{L}_{ij} \cdot (\boldsymbol{\sigma}_i - \boldsymbol{\sigma}_j) \Phi_{SOD} + i \mathbf{L}_{ij} \cdot (\boldsymbol{\sigma}_i \times \boldsymbol{\sigma}_j) \Phi_{SOX} + (3(\boldsymbol{\sigma}_i \cdot \hat{\mathbf{r}}_{ij})(\boldsymbol{\sigma}_j \cdot \hat{\mathbf{r}}_{ij}) - \boldsymbol{\sigma}_i \cdot \boldsymbol{\sigma}_j) \Phi_T \end{aligned} \quad (3)$$

with mass and energy parameters $m_{ij} = m_i m_j / (\epsilon_i + \epsilon_j)$ and $\epsilon_{ij} = ((\epsilon_i + \epsilon_j)^2 - m_i^2 - m_j^2) / (2(\epsilon_i + \epsilon_j))$, relative coordinate $\mathbf{r}_{ij} = \mathbf{r}_i - \mathbf{r}_j$, unit vector $\hat{\mathbf{r}}_{ij} = \mathbf{r}_{ij} / |\mathbf{r}_{ij}|$, and orbital and spin angular momenta \mathbf{L}_{ij} and $\boldsymbol{\sigma}_i$. The non-relativistic central potential $V_{q\bar{q}}(r)$ between a quark and its antiquark can be separated into two parts, $V_{q\bar{q}}(r) = A_{q\bar{q}}(r) + S_{q\bar{q}}(r)$, $A_{q\bar{q}}$ and $S_{q\bar{q}}$ control, respectively, the behavior of the potential at short and long distances. In vacuum one usually takes the Cornell potential [28], including a Coulomb part which dominates the wave function around $r = 0$ and a linear part which leads to the quark confinement, $A_{q\bar{q}}(r) = -\alpha_{q\bar{q}}/r$ and $S_{q\bar{q}}(r) = \sigma_{q\bar{q}} r$. For V_{qq} between two quarks one can take the similar separation,

$$\begin{aligned} V_{qq}(r) &= A_{qq}(r) + S_{qq}(r), \\ A_{qq}(r) &= -\alpha_{qq}/r, \\ S_{qq}(r) &= \sigma_{qq} r. \end{aligned} \quad (4)$$

If one considers only one gluon exchange, one obtains the Coulomb coupling constant $\alpha_{qq} = \alpha_{q\bar{q}}/2$ [29]. For the non-perturbative tensor strength σ which controls the degree of confinement, there is almost the same relation $\sigma_{qq} = \sigma_{q\bar{q}}/2$ from the recent lattice simulation [30]. All the relativistic corrections, including the Darwin term Φ_D , spin-spin coupling Φ_{SS} , spin-orbital couplings Φ_{SO} , Φ_{SOT} , Φ_{SOD} and Φ_{SOX} , and tensor coupling Φ_T , are explicitly shown in Appendix A. Note that, any Φ is a function of the distance $|\mathbf{r}_{ij}|$, the dependence of the potential on the azimuthal angles is reflected in the coefficients $H(\boldsymbol{\sigma}_i, \boldsymbol{\sigma}_j, \mathbf{L}_{ij}, \hat{\mathbf{r}}_{ij})$.

Solving the baryon mass M_b and wave function Ψ_b from the Schrödinger equation (1) is not a simple eigenstate problem, as the eigenvalue E or M_b appears also on the left hand side of the equation. We solve M_b or the binding energy $\mathcal{E} = M_b - M_q$ ($M_q = m_1 + m_2 + m_3$) by employing iteration method. For a given value $M_b^{(n)}$ at the n -th step, we first obtain the corresponding effective quark masses $\epsilon_i^{(n)}$ from the coupled equations (2), and then solve the Schrödinger equation (1) as an eigenstate problem with eigenvalue $E^{(n)}$. The baryon mass at the next step $M_b^{(n+1)} = \mathcal{E}^{(n+1)} + M_q$ is extracted from

$$\begin{aligned} \mathcal{E}^{(n+1)} &= \frac{1}{2} (\mathcal{E}^{(n)} + \bar{\mathcal{E}}), \\ \bar{\mathcal{E}} &= \frac{18E^{(n)}}{\sum_i (M_b^{(n)} + M_q)/\epsilon_i^{(n)}} + \frac{\sum_i m_i^2 - \sum_{i<j} m_i m_j}{(M_b^{(n)} + M_q)/2} - \sum_{i<j} \frac{\epsilon_i^{(n)} - \epsilon_j^{(n)}}{\epsilon_i^{(n)} + \epsilon_j^{(n)}} \frac{m_i^2 - m_j^2}{M_b^{(n)} + M_q}. \end{aligned} \quad (5)$$

With sufficiently large number of iteration steps, one could obtain the baryon mass up to arbitrary accuracy.

The iteration method employed here is different from the way used by Whitney *et al.* [25] where to simplify the calculation they took an approximate formula for the effective mass ϵ_i , instead of solving the coupled equations (2) self-consistently. This approximation will induce inaccuracy in solving the Schrödinger equation (1). We find that such approximation causes a shift of the baryon mass around $\lesssim 10$ MeV.

To effectively solve the Schrödinger-like equation for multi-body bound state problem, a usually used way is to expand the wave function in terms of known functions, such as hyperspherical harmonics [31, 32], Gaussian wave packets [33], and spherical harmonics [34]. The expansion depends strongly on the multi-body state. While in some special cases, for instance for ground state, one can take variational method and expand a ground state in terms of Gaussian wave packets [33] with different widths, a general and systematic study including both ground and excited states should be carried out in a complete and orthogonal Hilbert space.

We employ a numerical framework similar to Ref. [34] to treat the three-body bound state problem. We solve the baryon mass and wave function in the Hilbert space constructed by spherical harmonic oscillators which are by definition complete and orthogonal. Considering the mass difference among the three quarks in a general heavy flavor baryon, we take different constituent masses in constructing the spherical harmonic oscillators. This is different from Ref. [34] where all the three constituents are with the same mass. In such a framework we study both ground and excited states.

Like a two-body problem, we factorize the three-body motion into a center-of-mass motion and a relative motion. To this end, we introduce the coordinates \mathbf{R} for the center of mass and $\boldsymbol{\rho}$ and $\boldsymbol{\lambda}$ for the relative motion [31],

$$\begin{aligned}\mathbf{R} &= \frac{\epsilon_1 \mathbf{r}_1 + \epsilon_2 \mathbf{r}_2 + \epsilon_3 \mathbf{r}_3}{\epsilon_1 + \epsilon_2 + \epsilon_3}, \\ \boldsymbol{\rho} &= \sqrt{\frac{\epsilon_1 \epsilon_2}{(\epsilon_1 + \epsilon_2) \bar{m}}} (\mathbf{r}_1 - \mathbf{r}_2), \\ \boldsymbol{\lambda} &= \sqrt{\frac{\epsilon_3}{\bar{m}(\epsilon_1 + \epsilon_2)(\epsilon_1 + \epsilon_2 + \epsilon_3)}} [\epsilon_1 (\mathbf{r}_3 - \mathbf{r}_1) + \epsilon_2 (\mathbf{r}_3 - \mathbf{r}_2)],\end{aligned}\tag{6}$$

where \bar{m} is an arbitrary parameter with mass dimension and automatically disappears in the end and does not affect the result. Accordingly, we obtain the center-of-mass momentum and relative momenta

$$\begin{aligned}\mathbf{P} &= \mathbf{p}_1 + \mathbf{p}_2 + \mathbf{p}_3, \\ \mathbf{p} &= \sqrt{\frac{\bar{m} \epsilon_1 \epsilon_2}{\epsilon_1 + \epsilon_2}} \left(\frac{\mathbf{p}_1}{\epsilon_1} - \frac{\mathbf{p}_2}{\epsilon_2} \right), \\ \mathbf{q} &= \sqrt{\frac{\bar{m} \epsilon_3 (\epsilon_1 + \epsilon_2)}{\epsilon_1 + \epsilon_2 + \epsilon_3}} \left(-\frac{\mathbf{p}_1 + \mathbf{p}_2}{\epsilon_1 + \epsilon_2} + \frac{\mathbf{p}_3}{\epsilon_3} \right)\end{aligned}\tag{7}$$

and kinetic energy

$$\frac{\mathbf{p}_1^2}{2\epsilon_1} + \frac{\mathbf{p}_2^2}{2\epsilon_2} + \frac{\mathbf{p}_3^2}{2\epsilon_3} = \frac{\mathbf{P}^2}{2(\epsilon_1 + \epsilon_2 + \epsilon_3)} + \frac{\mathbf{p}^2 + \mathbf{q}^2}{2\bar{m}}.\tag{8}$$

After the coordinate transformation, the root-mean-squared baryon radius depends only on the relative coordinates,

$$\begin{aligned}r_{rms}^2 &= \frac{\epsilon_1 (\mathbf{r}_1 - \mathbf{R})^2 + \epsilon_2 (\mathbf{r}_2 - \mathbf{R})^2 + \epsilon_3 (\mathbf{r}_3 - \mathbf{R})^2}{\epsilon_1 + \epsilon_2 + \epsilon_3} \\ &= \frac{\epsilon_1 \epsilon_2 \mathbf{r}_{12}^2 + \epsilon_2 \epsilon_3 \mathbf{r}_{23}^2 + \epsilon_3 \epsilon_1 \mathbf{r}_{31}^2}{(\epsilon_1 + \epsilon_2 + \epsilon_3)^2} \\ &= \frac{\bar{m}}{\epsilon_1 + \epsilon_2 + \epsilon_3} (\boldsymbol{\rho}^2 + \boldsymbol{\lambda}^2).\end{aligned}\tag{9}$$

We now focus on the relative motion of the three-body problem which controls the inner structure of the bound state. We expand the relative wave function in terms of two-body spherical harmonic oscillators. For a single spherical harmonic oscillator, its stationary states are controlled by the Schrödinger equation

$$\left(-\frac{\hbar^2}{2\mu} \nabla^2 + \frac{\mu \omega^2}{2} r^2 \right) \Psi_{nlm}(\mathbf{r}) = E_{nl} \Psi_{nlm}(\mathbf{r})\tag{10}$$

with the energy levels $E_{nl} = (2n + l + 3/2)\hbar\omega$ and degenerated wave functions

$$\Psi_{nlm}(\mathbf{r}) = \psi_{nl}(r)Y_l^m(\theta, \phi) = \sqrt{\frac{2\Gamma(n+1)}{\Gamma(n+l+3/2)}}\alpha^{l+3/2}r^l e^{-\frac{\alpha^2 r^2}{2}} L_n^{l+1/2}(\alpha^2 r^2) Y_l^m(\theta, \varphi), \quad (11)$$

where n, l, m are respectively principal, orbital and magnetic quantum numbers, $\alpha = \sqrt{\mu\omega/\hbar}$ is the parameter characterizing the length scale of the quantum state, controlled by the frequency ω and mass μ of the oscillator, and $\Gamma(n)$, $L_n^{l+1/2}$, ψ_{nl} and Y_l^m are the Gamma functions, associated Laguerre polynomials and radial and spherical harmonic functions.

The two-body spherical harmonic oscillators are defined as a direct product of two single spherical harmonic oscillators,

$$|n_\rho l_\rho m_\rho n_\lambda l_\lambda m_\lambda\rangle = |n_\rho l_\rho m_\rho\rangle |n_\lambda l_\lambda m_\lambda\rangle \quad (12)$$

with the same scaling parameter α for the two oscillators.

Note that, the above defined two-body spherical harmonic oscillators are the exact solutions of a three-body bound state problem with interaction potential

$$\Phi(|\mathbf{r}_{ij}|) = \frac{\epsilon_i^2 \epsilon_j^2 \omega^2}{(\epsilon_i + \epsilon_j)(\epsilon_1 + \epsilon_2 + \epsilon_3)} r_{ij}^2 \quad (13)$$

with the scaling parameter $\alpha = \sqrt{m\omega/\hbar}$ and energy eigenvalues $E_{n_\rho n_\lambda l_\rho l_\lambda} = (2n_\rho + 2n_\lambda + l_\rho + l_\lambda + 3)\hbar\omega$. It has been tested that our numerical framework can reproduce the exact solution.

With the two-body spherical harmonic oscillators, we define the Hilbert space as a direct product of the flavor, spin and coordinate spaces,

$$|\Psi_{FSC}\rangle = |F\rangle \times |S\rangle \times |n_\rho l_\rho m_\rho n_\lambda l_\lambda m_\lambda\rangle. \quad (14)$$

The details on the flavor and spin states are shown in Appendix B. In such a Hilbert space we expand the baryon wave function

$$|\Psi_b\rangle = \sum_{FSC} C_{FSC} |\Psi_{FSC}\rangle. \quad (15)$$

Correspondingly, the Hamiltonian operator H of the system becomes a matrix in the Hilbert space,

$$H_{FSCF'S'C'} = \langle \Psi_{FSC} | H | \Psi_{F'S'C'} \rangle. \quad (16)$$

Taking into account the complete and orthogonal conditions for the states $|\Psi_{FSC}\rangle$, the eigenstate problem of a three-body system, $H |\Psi_b\rangle = E |\Psi_b\rangle$, becomes a matrix equation for the coefficients C_{FSC} ,

$$\sum_{F'S'C'} H_{FSCF'S'C'} C_{F'S'C'} = E C_{FSC}. \quad (17)$$

The Hamiltonian matrix can be further simplified through particle-index-rotation method. In the coordinate representation,

$$H_{FSCF'S'C'} = \int d^3\boldsymbol{\rho} d^3\boldsymbol{\lambda} \Psi_{n_\rho l_\rho m_\rho}^*(\boldsymbol{\rho}) \Psi_{n_\lambda l_\lambda m_\lambda}^*(\boldsymbol{\lambda}) \langle F | \langle S | K + W | F' \rangle | S' \rangle \Psi_{n'_\rho l'_\rho m'_\rho}(\boldsymbol{\rho}) \Psi_{n'_\lambda l'_\lambda m'_\lambda}(\boldsymbol{\lambda}). \quad (18)$$

The calculation for the kinetic energy $K = \sum_i p_i^2/(2\epsilon_i)$, which is proportional to $\nabla_\rho^2 + \nabla_\lambda^2$ after the transformation (8), is relative simple and the explicit expression is presented in Appendix D, the difficulty comes from the calculation for the potential part $W = \sum_{i<j} (\epsilon_i + \epsilon_j)/(2\epsilon_i \epsilon_j) \mathcal{V}_{ij}(\mathbf{r}_{ij})$. For the potential $\mathcal{V}_{12}(\mathbf{r}_{12})$ between the first and second constituents, since \mathbf{r}_{12} is proportional to $\boldsymbol{\rho}$ and independent of $\boldsymbol{\lambda}$, the six dimensional integration $\int d^3\boldsymbol{\rho} d^3\boldsymbol{\lambda}$ is reduced to a simple radial integration $\int \rho^2 d\rho$. For the other two potentials $\mathcal{V}_{23}(\mathbf{r}_{23})$ and $\mathcal{V}_{13}(\mathbf{r}_{13})$, since \mathbf{r}_{23} and \mathbf{r}_{13} depend on both $\boldsymbol{\rho}$ and $\boldsymbol{\lambda}$, the integration over $\boldsymbol{\rho}$ and $\boldsymbol{\lambda}$ can not be so simplified. We then make a rotation in the coordinate space from $(\boldsymbol{\rho}, \boldsymbol{\lambda})$ to $(\tilde{\boldsymbol{\rho}}, \tilde{\boldsymbol{\lambda}})$ to guarantee $\mathbf{r}_{23} \sim \tilde{\boldsymbol{\rho}}$ or $\mathbf{r}_{13} \sim \tilde{\boldsymbol{\rho}}$. This rotation in coordinate space is equivalent to a particle index rotation from the ordering $\{1, 2, 3\}$ to $\{2, 3, 1\}$ or $\{3, 1, 2\}$. The rotation can be explicitly written as

$$\Psi_{n_\rho l_\rho m_\rho}(\boldsymbol{\rho}) \Psi_{n_\lambda l_\lambda m_\lambda}(\boldsymbol{\lambda}) = \sum_{\tilde{n}_\rho \tilde{l}_\rho \tilde{m}_\rho \tilde{n}_\lambda \tilde{l}_\lambda \tilde{m}_\lambda} D_{\tilde{n}_\rho \tilde{l}_\rho \tilde{m}_\rho \tilde{n}_\lambda \tilde{l}_\lambda \tilde{m}_\lambda}^{n_\rho l_\rho m_\rho n_\lambda l_\lambda m_\lambda} \Psi_{\tilde{n}_\rho \tilde{l}_\rho \tilde{m}_\rho}(\tilde{\boldsymbol{\rho}}) \Psi_{\tilde{n}_\lambda \tilde{l}_\lambda \tilde{m}_\lambda}(\tilde{\boldsymbol{\lambda}}). \quad (19)$$

Benefited from the fact that, the total principal quantum number

$$N = 2n_\rho + 2n_\lambda + l_\rho + l_\lambda \quad (20)$$

and total magnetic quantum number

$$M = m_\rho + m_\lambda \quad (21)$$

are conserved under the rotation, the above expansion is finite and contains only limited terms. By taking such particle-index-rotation technique, the six dimensional integration in calculating the expectation values of \mathcal{V}_{23} and \mathcal{V}_{13} becomes again a simple radial integration $\int \tilde{\rho}^2 d\tilde{\rho}$. The details on the particle-index-rotation are given in Appendix C.

III. CONVERGENCY AND RESULTS

Before we numerically calculate the heavy flavor meson and baryon mass spectra and wave functions, we should first check the convergence of the expansion in terms of the two-body spherical harmonic oscillators. Note that, the completeness of the two-body oscillators $|n_\rho l_\rho m_\rho n_\lambda l_\lambda m_\lambda\rangle$ is independent of the value of the scaling parameter α , if we take infinite number of oscillators. When the number of the oscillators is finite in practical computation, the accuracy of the calculation depends on the choice of the α value.

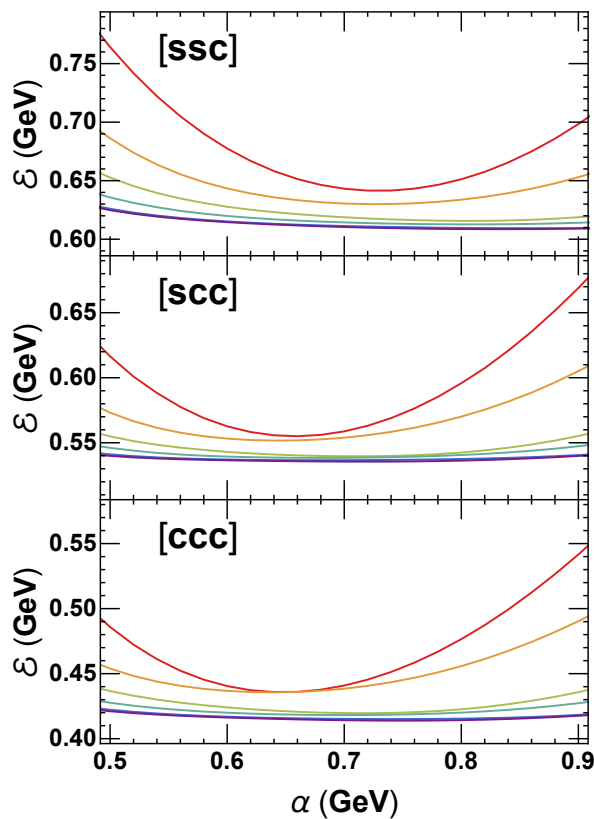


FIG. 1: The binding energy \mathcal{E} as a function of the scaling parameter α for singly, doubly and triply charmed baryon ground states $|ssc\rangle$, $|scc\rangle$ and $|ccc\rangle$. The six curves from top to bottom correspond to the maximal principal quantum number $N_{\max} = 0, 2, 4, 6, 8$ and 10 . The two curves with $N_{\max} = 8$ and 10 almost coincide.

For a baryon ground state, the α value corresponding to the most fast convergence can be fixed by applying variational method. We take α as a parameter and calculate the energy eigenvalue E and wave function Ψ_b as functions of α . By minimizing the eigenvalue

$$\frac{\partial E}{\partial \alpha} = 0, \quad \frac{\partial^2 E}{\partial \alpha^2} > 0, \quad (22)$$

we obtain the α value corresponding to the most fast convergence.

The number of the oscillators or the size of the Hilbert space is controlled by the maximum principal quantum number N_{\max} . We truncate the Hilbert space by taking the principle quantum number $N \leq N_{\max} = 0, 2, 4, 6, 8$ and 10. Considering the degeneracy of the wave functions, the corresponding number of oscillators is 1, 28, 210, 924, 3003 and 8008. From the parity symmetry which decouples states with odd and even N and momentum conservation which decouples states with different total magnetic quantum number M , the effective oscillators are reduced to 1, 8, 34, 108, 259 and 560. We first consider three specific baryon ground states $|ssc\rangle$, $|scc\rangle$ and $|ccc\rangle$ containing one, two and three charm quarks. We calculate their binding energy $\mathcal{E} = M_B - M_q$ and check its stability when N is large enough. The result is shown in Figure 1 for the three states and the six values of N_{\max} . With increasing N_{\max} , the α -dependence of \mathcal{E} becomes more and more smooth and reaches almost a constant for $N_{\max} = 8$ and 10. For the state $|ssc\rangle$, the minimum binding energy obtained from variational method is $\mathcal{E} = 0.642, 0.630, 0.616, 0.613, 0.610$ and 0.609 GeV corresponding to $\alpha = 0.72, 0.72, 0.80, 0.80, 0.84$ and 0.84 GeV, when N_{\max} increases from 0 to 10. For the other two states $|scc\rangle$ and $|ccc\rangle$, the α dependence is similar, but the binding energy reaches stability more fast. In the following calculation, we will take $N_{\max} = 10$ which already guarantees the stability of the numerical calculation.

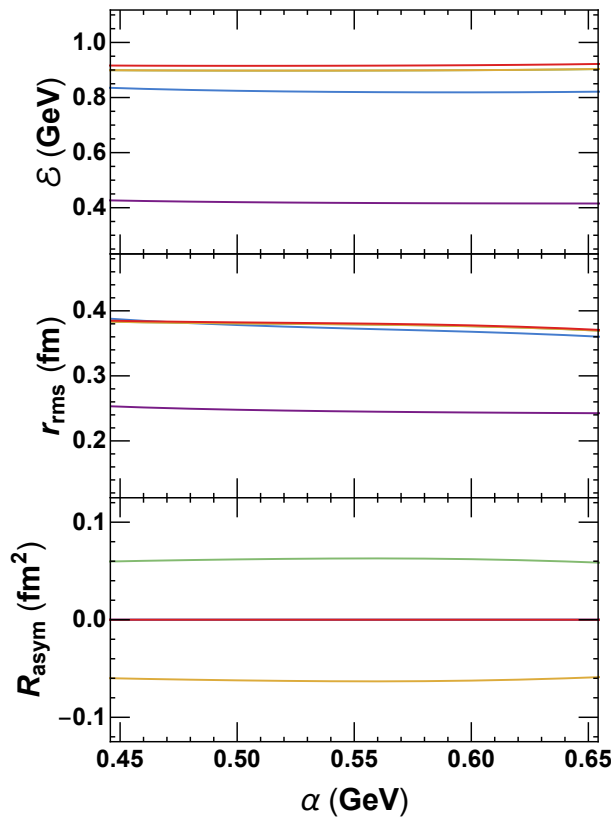


FIG. 2: The binding energy \mathcal{E} , mean radius r_{rms} and radius asymmetry R_{asym} as functions of the scaling parameter α for the triply charmed baryon states $|ccc\rangle$. The lines from top to bottom correspond to the ground and the first four excited states. The second and third excited states have degenerated \mathcal{E} , the second, third, and fourth excited states share the same r_{rms} , and R_{asym} is zero for the ground, first and fourth excited states.

Besides increasing the accuracy of calculating ground states, the other advantage to expand baryon wave functions in terms of a set of complete and orthogonal harmonic oscillators is to describe excited states. Since the variational method to find the most fast convergence fails in this case, we have to check carefully the α independence of the calculation. On the other hand, to describe the deviation of the inner structure of excited states from ground states and from an equilateral triangle, we should calculate not only the binding energy \mathcal{E} but also the root-mean-squared radius r_{rms} and the radius asymmetry R_{asym} . We take the excited states $|ccc\rangle$ as an example. For a baryon with three same quarks, r_{rms} and R_{asym} are reduced to $r_{rms} = \langle (r_{12}^2 + r_{23}^2 + r_{13}^2)/3 \rangle^{1/2}$ and $R_{asym} = \langle 2r_{12}^2 - r_{23}^2 - r_{13}^2 \rangle$. The results for the ground and first four excited states of $|ccc\rangle$ with $N_{\max} = 10$ are shown in Figure 2. In the region of $0.45 < \alpha < 0.65$, they are almost constants. Considering the degeneracy of the baryon states and the symmetry among the three quarks, the binding energies for the second and third excited states are the same, the second, third,

and fourth excited states share the same mean radius, and the radius asymmetry is zero for the ground, first and fourth excited states.

With the tested expansion method, we now compute the heavy flavor hadron states by the two- [22–24, 26, 27] and 3-body Dirac Equations. We employ the Cornell potential to describe the quark-antiquark and quark-quark interactions for mesons and baryons. To self-consistently describe both the meson and baryon states and to extend the multi-body Dirac equations to further study of other new multi-quark states, we take a universal set of parameters, by fitting the heavy flavor meson and baryon masses. The parameters we used, including the vacuum quark masses and coupling strengths α and σ , are shown in Table I.

$m_u = m_d = 0.150 \text{ GeV}$
$m_s = 0.301 \text{ GeV}$
$m_c = 1.458 \text{ GeV}$
$m_b = 4.824 \text{ GeV}$
$\alpha_{q\bar{q}} = 2\alpha_{qq} = 0.50$
$\sigma_{q\bar{q}} = 2\sigma_{qq} = 0.17 \text{ GeV}^2$

TABLE I: The universal set of parameters for heavy flavor mesons and baryons.

Meson	J^P	M_E (GeV)	M_T (GeV)	D_R	r_{rms} (fm)
D^0	0^-	1.865	1.908	2.3%	0.41
D^{*0}	1^-	2.007	2.057	2.5%	0.48
D^+	0^-	1.870	1.908	2.0%	0.41
D^{*+}	1^-	2.010	2.057	2.3%	0.48
D_s	0^-	1.968	2.006	1.9%	0.39
D_s^*	1^-	2.112	2.165	2.5%	0.46
η_c	0^-	2.984	2.966	0.6%	0.29
$\eta_c(2S)$	0^-	3.637	3.580	1.6%	0.63
h_{c1}	1^+	3.525	3.525	0.0%	0.55
J/ψ	1^-	3.097	3.149	1.7%	0.37
ψ	1^-	3.686	3.697	0.3%	0.69
χ_{c0}	0^+	3.415	3.440	0.7%	0.47
χ_{c1}	1^+	3.511	3.520	0.3%	0.54
χ_{c2}	2^+	3.556	3.542	0.4%	0.57
B^-	0^-	5.279	5.310	0.2%	0.44
B^{*-}	1^-	5.325	5.365	0.8%	0.47
B^0	0^-	5.280	5.310	0.6%	0.44
B^{0*}	1^-	5.325	5.365	0.8%	0.47
B_s	0^-	5.367	5.402	0.7%	0.41
B_s^*	1^-	5.415	5.467	1.0%	0.44
η_b	0^-	9.399	9.284	1.2%	0.16
$\eta_b(2S)$	0^-	9.999	9.948	0.5%	0.42
h_{b1}	1^+	9.899	9.939	0.4%	0.37
$\Upsilon(1S)$	1^-	9.460	9.500	0.4%	0.21
$\Upsilon(2S)$	1^-	10.023	10.031	0.1%	0.47
χ_{b0}	0^+	9.859	9.887	0.3%	0.33
χ_{b1}	1^+	9.893	9.932	0.4%	0.37
χ_{b2}	2^+	9.912	9.953	0.4%	0.38

TABLE II: Experimentally measured [35] and model calculated heavy flavor meson masses M_E and M_T . $D_R = |(M_T - M_E)/M_E|$ is the relative difference, and r_{rms} is the root-mean-squared radius calculated from the meson wave function.

The calculated heavy flavor meson mass M_T and the comparison with the experimentally measured mass M_E [35]

are shown in Table II. With the relative part of the meson wave function $\Psi_m(\mathbf{r})$, we present also the root-mean-squared radius $r_{rms}^2 = \int d^3\mathbf{r} r^2 \Psi_m^\dagger(\mathbf{r}) \Psi_m(\mathbf{r})$. From the relative difference $D_R = |(M_T - M_E)/M_E| < 2.5\%$ between the data and model calculation, the two-body Dirac equation describes heavy flavor mesons very well, especially for closed heavy flavors and bottomed heavy flavors.

Baryon	J^P	M_E (GeV)	M_T (GeV)	D_R
Λ_c^+	$(1/2)^+$	2.286	2.383	4.2%
Σ_c^{++}	$(1/2)^+$	2.454	2.356	4.0%
Σ_c^+	$(1/2)^+$	2.453	2.356	4.0%
Σ_c^0	$(1/2)^+$	2.454	2.356	4.0%
Ξ_c^+	$(1/2)^+$	2.468	2.517	1.9%
Ξ_c^0	$(1/2)^+$	2.471	2.517	1.8%
$\Xi_c'^+$	$(1/2)^+$	2.577	2.532	1.8%
$\Xi_c'^0$	$(1/2)^+$	2.579	2.532	1.9%
Ω_c^0	$(1/2)^+$	2.695	2.660	1.3%
Ξ_{cc}^{++}	$(1/2)^+$	3.621	3.616	0.1%
Ξ_{cc}^+	$(1/2)^+$	3.619	3.616	0.1%
Ω_{cc}^+	$(1/2)^+$		3.746	
Σ_c^{*++}	$(3/2)^+$	2.518	2.369	6.3%
Σ_c^{*+}	$(3/2)^+$	2.518	2.369	6.3%
Σ_c^{*0}	$(3/2)^+$	2.518	2.369	6.3%
Ξ_c^{*+}	$(3/2)^+$	2.646	2.527	4.5%
Ξ_c^{*0}	$(3/2)^+$	2.646	2.527	4.5%
Ω_c^{*0}	$(3/2)^+$	2.766	2.669	3.5%
Ξ_{cc}^{*++}	$(3/2)^+$		3.627	
Ξ_{cc}^{*+}	$(3/2)^+$		3.627	
Ω_{cc}^{*+}	$(3/2)^+$		3.754	
Ω_{ccc}^{*+}	$(3/2)^+$		4.790	
Λ_b^0	$(1/2)^+$	5.620	5.744	2.3%
Σ_b^+	$(1/2)^+$	5.811	5.720	1.5%
Σ_b^0	$(1/2)^+$		5.720	
Σ_b^-	$(1/2)^+$	5.816	5.720	1.6%
Ξ_b^0	$(1/2)^+$	5.792	5.871	1.4%
Ξ_b^-	$(1/2)^+$	5.795	5.871	1.3%
Ω_b^-	$(1/2)^+$	6.046	6.007	0.6%
Ξ_{bb}^+	$(1/2)^+$		10.195	
Ξ_{bb}^0	$(1/2)^+$		10.195	
Ω_{bb}^-	$(1/2)^+$		10.318	
Σ_b^{*+}	$(3/2)^+$	5.832	5.736	1.6%
Σ_b^{*0}	$(3/2)^+$		5.736	
Σ_b^{*-}	$(3/2)^+$	5.835	5.736	1.6%
Ξ_b^{*0}	$(3/2)^+$		5.886	
Ξ_b^{*-}	$(3/2)^+$		5.886	
Ω_b^{*-}	$(3/2)^+$		6.021	
Ξ_{bb}^{*+}	$(3/2)^+$		10.210	
Ξ_{bb}^{*0}	$(3/2)^+$		10.210	
Ω_{bb}^{*-}	$(3/2)^+$		10.332	
Ω_{bbb}^-	$(3/2)^+$		14.440	

TABLE III: Experimentally measured [35] and model calculated heavy flavor baryon masses M_E and M_T . D_R is the relative difference between the data and our calculation.

We now turn to calculate the heavy flavor baryon states with the three-body Dirac equation. The baryon masses and the comparison with the experimental data are shown in Table III. For doubly charmed and singly bottomed baryons which have been observed experimentally, the agreement between the calculation and the data is good enough with relative difference $D_R < 2.3\%$. Theoretically, we expect that, the relativistic potential model is even better to describe triply charmed and doubly and triply bottomed baryons. For singly charmed baryons, however, the model calculation is not so good. Especially for those baryons with two light quarks u and d , the relative difference for some states reaches 6.3%. This is due to the fact that, the creation-annihilation fluctuations for light quarks may play a sizable role, and the interaction between two light quarks can not fully described by a potential. It is phenomenologically suggested that [36], a three body force $C/(m_1 m_2 m_3)$ controlled by the constituent quark masses may improve the calculation for heavy flavor baryons, especially for the baryons with two light quarks. From the comparison with the calculation by Whitney *et al* [25] where the parameters for baryons are different from the ones for mesons, the quality of our calculation with a universal set of parameters for both mesons and baryons is only slightly reduced, the relative difference increases from $D_R < 4.2\%$ to 6.3%.

Baryon	Experiment		Model		D_R
	J^P	M_E (GeV)	J^P	M_T (GeV)	
Ω_c^0	$(1/2)^+$	2.695	$(1/2)^+ (1S)$	2.660	1.3%
$\Omega_c^*(2770)^0$	$(3/2)^+$	2.766	$(3/2)^+ (1S)$	2.669	3.5%
$\Omega_c(3000)^0$		3.000	$(1/2)^- (1P)$	2.965	1.2%
$\Omega_c(3050)^0$		3.050	$(3/2)^- (1P)$	3.042	0.3%
$\Omega_c(3065)^0$		3.065	$(1/2)^- (1P)$	3.053	0.3%
$\Omega_c(3090)^0$		3.090	$(3/2)^- (1P)$	3.220	4.2%
$\Omega_c(3120)^0$		3.119	$(5/2)^- (1P)$	3.292	5.5%

TABLE IV: Experimentally measured and model calculated ground states and excited states of Ω_c .

With the expansion method in a complete and orthogonal Hilbert space, we can calculate not only the baryon ground states but also the excited states. Table IV shows the result for $\Omega_c[ssc]$. Ω_c^0 and $\Omega_c^*(2770)^0$ are the ground states with $J^P = (1/2)^+$ and $(3/2)^+$, and the other five baryons are excited states. Their masses have been experimentally measured but the total spins and parities are not yet fixed. From our model calculation, they are all $1P$ states with $J^P = (1/2)^-, (3/2)^-$ and $(5/2)^-$. The mass difference among them is mainly from the spin-orbit and spin-spin interactions. The expansion method in our calculation gives almost the same accuracy as for the ground states, the relative difference for the mass is $D_R < 5.5\%$.

The solution of the three-body Dirac equation provides not only the baryon mass but also the wave function which controls the baryon structure like mean mass radius, mean charge radius and even magnetic moment [36]. We focus here on the mass-weighted mean radius of the baryon and averaged distance between any two quarks, the former controls the coalescence probability in quark coalescence models [37, 38] in high energy nuclear collisions, and the latter characterizes the inner structure of the baryon. The root-mean-squared radius $r_{rms} = M_b^{-1} \langle \sum_{i < j} \epsilon_i \epsilon_j r_{ij}^2 \rangle^{1/2}$ which is equivalent to (9) and the mean distances $\langle r_{ij}^2 \rangle^{1/2}$ between quark i and quark j are shown in Table V. To be specific, we label the three quarks with index 1 for the lightest one and 3 for the heaviest one. For instance, $\langle r_{12}^2 \rangle^{1/2}$, $\langle r_{13}^2 \rangle^{1/2}$ and $\langle r_{23}^2 \rangle^{1/2}$ mean respectively $\langle r_{us}^2 \rangle^{1/2}$, $\langle r_{uc}^2 \rangle^{1/2}$ and $\langle r_{sc}^2 \rangle^{1/2}$ for Ξ_c . It is easy to see the relation $\langle r_{12}^2 \rangle^{1/2} \geq \langle r_{13}^2 \rangle^{1/2} \geq \langle r_{23}^2 \rangle^{1/2}$, it means that, light quarks are loosely bounded in comparison with heavy quarks. Note that, the mean distance between two charm quarks is 0.45 fm for Ω_{cc} and 0.42 fm for Ω_{ccc} which are both larger than the mean radius $r_{rms} = 0.37$ fm for J/ψ shown in Table II. This reflects the fact that the quark-quark potential is

Baryon	r_{rms}	$\langle r_{12}^2 \rangle^{1/2}$	$\langle r_{13}^2 \rangle^{1/2}$	$\langle r_{23}^2 \rangle^{1/2}$
$\Lambda_c^+, \Sigma_c, \Sigma_c^*$	0.29	0.58	0.56	0.56
Ξ_c, Ξ_c^*	0.29	0.58	0.55	0.54
$\Omega_c^0, \Omega_c^{*0}$	0.29	0.57	0.53	0.53
Ξ_{cc}, Ξ_{cc}^*	0.28	0.56	0.56	0.45
$\Omega_{cc}^{++}, \Omega_{cc}^{*++}$	0.27	0.53	0.53	0.44
Ω_{ccc}^{+++}	0.24	0.42	0.42	0.42

TABLE V: The root-mean-squared radius and averaged distance between any two quarks for charmed baryons. The unit is fm. The three quarks are labeled with index 1 for the lightest one and 3 for the heaviest one.

only one half of the quark-antiquark potential.

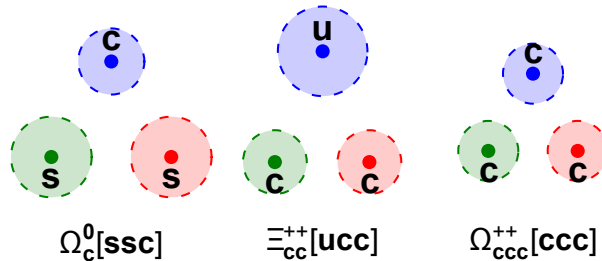


FIG. 3: Averaged configuration of singly, doubly and triply charmed baryons.

To have a vivid picture of the structure of heavy flavor baryons, we plot the averaged configuration of singly, doubly and triply charmed baryons Ω_c^0 , Ξ_{cc}^{++} and Ω_{ccc}^{++} in Figure 3. The distance between the centers of two quarks is described by $\langle r_{ij}^2 \rangle^{1/2}$, and the effective moving region of a quark Δr_i is controlled by the variation of the quark distances $(\Delta r_i)^2 + (\Delta r_j)^2 = \langle r_{ij}^2 \rangle - \langle r_{ij} \rangle^2$. While for Ξ_{cc}^{++} the distance difference between light-heavy and heavy-heavy quarks reaches $\langle r_{uc}^2 \rangle^{1/2} - \langle r_{cc}^2 \rangle^{1/2} = (0.56 - 0.45) \text{ fm} = 0.21 \text{ fm}$, all the baryon configurations are not far from an equilateral triangle, and the quark-diquark structure is hardly applicable even for Ξ_{cc}^{++} . The way using wave function to analyze hadron inner structure is helpful in the future study of four-quark and five-quark systems to distinguish tetraquark and pentaquark states from molecule states.

IV. SUMMARY

We improved the method to solve the three-body Dirac equation for heavy flavor baryons. We expanded the baryon wave function in the Hilbert space constructed by complete and orthogonal spherical harmonic oscillators, and employed the particle-index-rotation technique to reduce the integration dimension in calculating the Hamiltonian matrix elements. These improvements increase the accuracy and stability of solving the Dirac equation and extend the calculation to baryon excited states.

In the improved framework, we systematically solved the two- and three-body Dirac equations for heavy flavor mesons and baryons. Since in the Dirac equations the spin interaction terms, including all possible spin-orbital and spin-spin couplings, are self-consistently involved in the two-body potential, we calculated the mass spectra and quark distributions for all the heavy flavor ground states and predicted the total spin and parity of those unobserved baryon excited states. Unlike the previous calculations with different mass parameters for mesons and baryons, we took a universal set of parameters for both mesons and baryons. This makes the calculation more self-consistent and predictable for future studies of multi-quark states. From the comparison with the experimental data, the relative difference between the model calculated and experimentally observed hadron masses is less than 2.5% for mesons and 6.3% for baryons. Note that, if we give up the self-consistency and prediction power and take different parameter sets for mesons and baryons, the relative difference between model calculation and experimental data will be sizeably reduced.

The improved method can directly be applied to studying heavy flavor hadrons in hot medium, by taking into account the lattice simulated medium correction to the interaction potential [39, 40]. Combining with the quark coalescence mechanism, we can calculate the hadron distributions in the final state, like production rate, momentum spectra, and azimuthal anisotropy in high energy nuclear collisions [12–14, 41]. Another application is to extend the relativistic three-body potential model to including more quarks. This would be a valuable tool to quantitatively study the properties of heavy flavor tetraquark and pentaquark bound states.

Acknowledgement: We thank Mr. Tiecheng Guo for the collaboration in the beginning of this work, and Profs. Charles Gale and Sangyong Jeon for helpful discussions. JZ and PZ are supported by the NSFC grant Nos. 11575093 and 11890712, and SS is grateful to the Natural Sciences and Engineering Research Council of Canada.

Appendix A: Relativistic Two-body interactions

The Darwin term, spin-spin and spin-orbital couplings in the relativistic potential (3) between two quarks are defined as [22–24]

$$\begin{aligned}
\Phi_D &= B - \frac{2F'(\cosh 2K - 1)}{r} + F'^2 + K'^2 + \frac{2K' \sinh 2K}{r} - \nabla^2 F - \frac{2(\cosh 2K - 1)}{r^2}, \\
\Phi_{SS} &= Q + \frac{2K' \sinh 2K}{3r} - \frac{2F'(\cosh 2K - 1)}{3r} - \frac{2(\cosh 2K - 1)}{3r^2} + \frac{2F'K'}{3} - \frac{\nabla^2 K}{3}, \\
\Phi_{SO} &= -\frac{F'}{r} - \frac{F'(\cosh 2K - 1)}{r} - \frac{\cosh 2K - 1}{r^2} + \frac{K' \sinh 2K}{r}, \\
\Phi_{SOT} &= -\frac{K' \cosh 2K}{r} + \frac{\sinh 2K}{r^2} + \frac{F' \sinh 2K}{r}, \\
\Phi_{SOD} &= O \cosh 2K - P \sinh 2K, \\
\Phi_{SOX} &= P \cosh 2K - O \sinh 2K, \\
\Phi_T &= \frac{1}{3} \left[R + \frac{3F' \sinh 2K}{r} + \frac{F'(\cosh 2K - 1)}{r} + 2F'K' - \frac{K' \sinh 2K}{r} - \frac{3K'(\cosh 2K - 1)}{r} \right. \\
&\quad \left. - \nabla^2 K + \frac{3 \sinh 2K}{r^2} + \frac{\cosh 2K - 1}{r^2} \right]
\end{aligned} \tag{A1}$$

with

$$\begin{aligned}
B &= -\frac{1}{2} \nabla^2 G + \frac{3}{4} G'^2 + G'F' - K'^2, \\
G &= -\frac{1}{2} \ln [1 - 2A/(\epsilon_i + \epsilon_j)], \\
F &= \frac{1}{2} \ln \frac{E_i M_j + E_j M_i}{\epsilon_j m_i + \epsilon_i m_j} - G, \\
K &= \frac{G + L}{2}, \\
L &= \ln \left[\frac{\sqrt{m_i^2 + (2m_{ij}S + S^2)/(1 - 2A/(\epsilon_i + \epsilon_j))}}{m_i + m_j} + \frac{\sqrt{m_j^2 + (2m_{ij}S + S^2)/(1 - 2A/(\epsilon_i + \epsilon_j))}}{m_i + m_j} \right], \\
O &= -\frac{1}{2r} \frac{E_j M_j - E_i M_i}{E_j M_i + E_i M_j} (L' - G'), \\
P &= \frac{1}{2r} \frac{E_i M_j - E_j M_i}{E_j M_i + E_i M_j} (L' - G'), \\
Q &= \frac{1}{3} \nabla^2 (K + G) - \frac{2F'(G' + K')}{3} - \frac{1}{2} G'^2, \\
R &= \nabla^2 K - \frac{1}{2} \nabla^2 G + \frac{3(G' - 2K')}{2r} + F'(G' - 2K')
\end{aligned} \tag{A2}$$

and

$$\begin{aligned}
M_i &= m_i \cosh L + m_j \sinh L, \\
M_j &= m_j \cosh L + m_i \sinh L, \\
E_i &= \epsilon_i \cosh G - \epsilon_j \sinh G, \\
E_j &= \epsilon_j \cosh G - \epsilon_i \sinh G,
\end{aligned} \tag{A3}$$

where F', G', K' and L' are derivatives of F, G, K and L with respect to r .

Appendix B: Flavor and spin states

For baryons containing only one flavor, one has only the symmetric flavor state,

$$|F\rangle_S = |qqq\rangle. \tag{B1}$$

For baryons with two flavors, one can construct both symmetric and mixed symmetric and antisymmetric states,

$$\begin{aligned} |F\rangle_S &= [|qqq'\rangle + |qq'q\rangle + |q'qq\rangle] / \sqrt{3}, \\ |F\rangle_{MS} &= [2|qqq'\rangle - |qq'q\rangle - |q'qq\rangle] / \sqrt{6}, \\ |F\rangle_{MA} &= [|qq'q\rangle - |q'qq\rangle] / \sqrt{2}. \end{aligned} \quad (B2)$$

For baryons with three different flavors, all symmetric, antisymmetric, mixed symmetric and mixed antisymmetric states can be constructed,

$$\begin{aligned} |F\rangle_S &= [|q_1q_2q_3\rangle + |q_2q_1q_3\rangle + |q_2q_3q_1\rangle + |q_3q_2q_1\rangle + |q_3q_1q_2\rangle + |q_1q_3q_2\rangle] / \sqrt{6}, \\ |F\rangle_A &= [|q_1q_2q_3\rangle - |q_2q_1q_3\rangle + |q_2q_3q_1\rangle - |q_3q_2q_1\rangle + |q_3q_1q_2\rangle - |q_1q_3q_2\rangle] / \sqrt{6}, \\ |F\rangle_{MS1} &= [-2|q_1q_2q_3\rangle - 2|q_2q_1q_3\rangle + |q_2q_3q_1\rangle + |q_3q_2q_1\rangle + |q_3q_1q_2\rangle + |q_1q_3q_2\rangle] / \sqrt{12}, \\ |F\rangle_{MA1} &= [|q_2q_3q_1\rangle - |q_3q_2q_1\rangle - |q_3q_1q_2\rangle + |q_1q_3q_2\rangle] / \sqrt{4}, \\ |F\rangle_{MS2} &= [|q_2q_3q_1\rangle + |q_3q_2q_1\rangle - |q_3q_1q_2\rangle - |q_1q_3q_2\rangle] / \sqrt{4}, \\ |F\rangle_{MA2} &= [-2|q_1q_2q_3\rangle + 2|q_2q_1q_3\rangle + |q_2q_3q_1\rangle - |q_3q_2q_1\rangle + |q_3q_1q_2\rangle - |q_1q_3q_2\rangle] / \sqrt{12}. \end{aligned} \quad (B3)$$

Note that, the symmetry of $|F\rangle_{MS1}$ and $|F\rangle_{MA1}$ and antisymmetry of $|F\rangle_{MS2}$ and $|F\rangle_{MA2}$ are in the sense of the flavor exchange between the first two quarks $q_1 \leftrightarrow q_2$, corresponding to isospin triplet and singlet for $q_1, q_2 = u, d$.

Considering only two spin eigenstates $|s_z\rangle = |\pm 1/2\rangle$ for a fermion, the spin states of a baryon are similar to its flavor states with two flavors,

$$\begin{aligned} |S\rangle_{S1} &= |1/2, 1/2, 1/2\rangle, \\ |S\rangle_{S2} &= |-1/2, -1/2, -1/2\rangle, \\ |S\rangle_{S3} &= [|1/2, 1/2, -1/2\rangle + |1/2, -1/2, 1/2\rangle + |-1/2, 1/2, 1/2\rangle] / \sqrt{3}, \\ |S\rangle_{S4} &= [|-1/2, -1/2, 1/2\rangle + |-1/2, 1/2, -1/2\rangle + |1/2, -1/2, -1/2\rangle] / \sqrt{3}, \\ |S\rangle_{MS1} &= [2|1/2, 1/2, -1/2\rangle - |1/2, -1/2, 1/2\rangle - |-1/2, 1/2, 1/2\rangle] / \sqrt{6}, \\ |S\rangle_{MS2} &= [2|-1/2, -1/2, 1/2\rangle - |-1/2, 1/2, -1/2\rangle - |1/2, -1/2, -1/2\rangle] / \sqrt{6}, \\ |S\rangle_{MA1} &= [|1/2, -1/2, 1/2\rangle - |-1/2, 1/2, 1/2\rangle] / \sqrt{2}, \\ |S\rangle_{MA2} &= [|-1/2, 1/2, -1/2\rangle - |1/2, -1/2, -1/2\rangle] / \sqrt{2}, \end{aligned} \quad (B4)$$

where the mixed symmetry (MS) and mixed antisymmetry (MA) are with respect to the spin exchange of the first two quarks.

Appendix C: Particle index rotation

In order to solve the Schrödinger-like equation (1) in the Hilbert space constructed by spherical harmonic oscillators, we need to compute the potential matrix element $\langle n'_\rho l'_\rho m'_\rho n'_\lambda l'_\lambda m'_\lambda | \Phi(|\mathbf{r}_{ij}|) | n_\rho l_\rho m_\rho n_\lambda l_\lambda m_\lambda \rangle$. The integration is simpler for $\Phi(|\mathbf{r}_{12}|)$ as $\boldsymbol{\rho}$ is proportional to \mathbf{r}_{12} and hence the six dimensional integration $\int d^3\boldsymbol{\rho} d^3\boldsymbol{\lambda}$ is simplified as a radial integration $\int \rho^2 d\rho$. However, the integrations for $\Phi(|\mathbf{r}_{23}|)$ and $\Phi(|\mathbf{r}_{13}|)$ are not so easy, since \mathbf{r}_{23} and \mathbf{r}_{13} depend on both $\boldsymbol{\rho}$ and $\boldsymbol{\lambda}$. To avoid complicated six dimensional integrations which may reduce the accuracy of the computation, we take a coordinate transformation from $(\boldsymbol{\rho}, \boldsymbol{\lambda})$ to $(\tilde{\boldsymbol{\rho}}, \tilde{\boldsymbol{\lambda}})$ where \mathbf{r}_{23} or \mathbf{r}_{13} is proportional to $\tilde{\boldsymbol{\rho}}$.

The new coordinates $(\tilde{\boldsymbol{\rho}}, \tilde{\boldsymbol{\lambda}})$ are defined through a rotation,

$$\begin{bmatrix} \tilde{\boldsymbol{\rho}} \\ \tilde{\boldsymbol{\lambda}} \end{bmatrix} = \begin{bmatrix} \cos \theta & \sin \theta \\ -\sin \theta & \cos \theta \end{bmatrix} \begin{bmatrix} \boldsymbol{\rho} \\ \boldsymbol{\lambda} \end{bmatrix}. \quad (C1)$$

Taking into account the expressions of \mathbf{r}_{13} and \mathbf{r}_{23} in terms of the relative coordinates $\boldsymbol{\rho}$ and $\boldsymbol{\lambda}$,

$$\begin{aligned} \sqrt{\frac{\epsilon_2 \epsilon_3}{(\epsilon_2 + \epsilon_3) \bar{m}}} (\mathbf{r}_2 - \mathbf{r}_3) &= -\sqrt{\frac{\epsilon_1 \epsilon_3}{(\epsilon_1 + \epsilon_2)(\epsilon_2 + \epsilon_3)}} \boldsymbol{\rho} - \sqrt{\frac{\epsilon_2(\epsilon_1 + \epsilon_2 + \epsilon_3)}{(\epsilon_1 + \epsilon_2)(\epsilon_2 + \epsilon_3)}} \boldsymbol{\lambda}, \\ \sqrt{\frac{\epsilon_3 \epsilon_1}{(\epsilon_3 + \epsilon_1) \bar{m}}} (\mathbf{r}_3 - \mathbf{r}_1) &= -\sqrt{\frac{\epsilon_2 \epsilon_3}{(\epsilon_1 + \epsilon_2)(\epsilon_3 + \epsilon_1)}} \boldsymbol{\rho} + \sqrt{\frac{\epsilon_1(\epsilon_1 + \epsilon_2 + \epsilon_3)}{(\epsilon_1 + \epsilon_2)(\epsilon_3 + \epsilon_1)}} \boldsymbol{\lambda}, \end{aligned} \quad (C2)$$

the rotation angle θ_{13} or θ_{23} is fixed by the condition $\mathbf{r}_{13} \sim \tilde{\boldsymbol{\rho}}$ or $\mathbf{r}_{23} \sim \tilde{\boldsymbol{\rho}}$. Corresponding to the rotation, the two-body spherical harmonic oscillator $\Psi_{n_\rho l_\rho m_\rho}(\boldsymbol{\rho})\Psi_{n_\lambda l_\lambda m_\lambda}(\boldsymbol{\lambda})$ becomes $\Psi_{\tilde{n}_\rho \tilde{l}_\rho \tilde{m}_\rho}(\tilde{\boldsymbol{\rho}})\Psi_{\tilde{n}_\lambda \tilde{l}_\lambda \tilde{m}_\lambda}(\tilde{\boldsymbol{\lambda}})$ through the transformation (19). When calculating the coefficients $D_{\tilde{n}_\rho \tilde{l}_\rho \tilde{m}_\rho \tilde{n}_\lambda \tilde{l}_\lambda \tilde{m}_\lambda}^{n_\rho l_\rho m_\rho n_\lambda l_\lambda m_\lambda}[\theta]$, the total energy and total angular momentum conservation

$$\begin{aligned} N &= 2n_\rho + 2n_\lambda + l_\rho + l_\lambda = 2\tilde{n}_\rho + 2\tilde{n}_\lambda + \tilde{l}_\rho + \tilde{l}_\lambda, \\ M &= m_\rho + m_\lambda = \tilde{m}_\rho + \tilde{m}_\lambda \end{aligned} \quad (\text{C3})$$

helps a lot to reduce the Hilbert space.

Appendix D: Hamiltonian matrix elements

With the known transformation coefficients in coordinate space, we are now ready to write down explicitly the Hamiltonian matrix elements in the Hilbert space.

1. Kinetic energy and root-mean-squared radius

Let's first consider the elements of the baryon kinetic energy and root-mean-squared radius. From their expressions (8) and (9), they can be directly calculated without coordinate transformation. Taking into account the orthogonality of the spherical harmonic oscillators,

$$\langle n'_\rho l'_\rho m'_\rho n'_\lambda l'_\lambda m'_\lambda | n_\rho l_\rho m_\rho n_\lambda l_\lambda m_\lambda \rangle = \delta_{n'_\rho}^{n_\rho} \delta_{l'_\rho}^{l_\rho} \delta_{m'_\rho}^{m_\rho} \delta_{n'_\lambda}^{n_\lambda} \delta_{l'_\lambda}^{l_\lambda} \delta_{m'_\lambda}^{m_\lambda}, \quad (\text{D1})$$

the elements for the kinetic energy are clearly expressed as

$$\begin{aligned} &\langle n'_\rho l'_\rho m'_\rho n'_\lambda l'_\lambda m'_\lambda | -\nabla_\rho^2 | n_\rho l_\rho m_\rho n_\lambda l_\lambda m_\lambda \rangle \\ &= \delta_{l'_\rho}^{l_\rho} \delta_{m'_\rho}^{m_\rho} \delta_{n'_\lambda}^{n_\lambda} \delta_{l'_\lambda}^{l_\lambda} \delta_{m'_\lambda}^{m_\lambda} \alpha^2 \left[(2n_\rho + l_\rho + 3/2) \delta_{n'_\rho}^{n_\rho} + \sqrt{n_\rho(n_\rho + l_\rho + 1/2)} \delta_{n'_\rho}^{n_\rho+1} + \sqrt{(n_\rho + 1)(n_\rho + l_\rho + 3/2)} \delta_{n'_\rho}^{n_\rho-1} \right], \\ &\langle n'_\rho l'_\rho m'_\rho n'_\lambda l'_\lambda m'_\lambda | -\nabla_\lambda^2 | n_\rho l_\rho m_\rho n_\lambda l_\lambda m_\lambda \rangle \\ &= \delta_{n'_\rho}^{n_\rho} \delta_{l'_\rho}^{l_\rho} \delta_{m'_\rho}^{m_\rho} \delta_{l'_\lambda}^{l_\lambda} \delta_{m'_\lambda}^{m_\lambda} \alpha^2 \left[(2n_\lambda + l_\lambda + 3/2) \delta_{n'_\lambda}^{n_\lambda} + \sqrt{n_\lambda(n_\lambda + l_\lambda + 1/2)} \delta_{n'_\lambda}^{n_\lambda+1} + \sqrt{(n_\lambda + 1)(n_\lambda + l_\lambda + 3/2)} \delta_{n'_\lambda}^{n_\lambda-1} \right], \end{aligned} \quad (\text{D2})$$

and similarly we have the elements for the root-mean-squared radius,

$$\begin{aligned} &\langle n'_\rho l'_\rho m'_\rho n'_\lambda l'_\lambda m'_\lambda | \rho^2 | n_\rho l_\rho m_\rho n_\lambda l_\lambda m_\lambda \rangle \\ &= \delta_{l'_\rho}^{l_\rho} \delta_{m'_\rho}^{m_\rho} \delta_{n'_\lambda}^{n_\lambda} \delta_{l'_\lambda}^{l_\lambda} \delta_{m'_\lambda}^{m_\lambda} \alpha^{-2} \left[(2n_\rho + l_\rho + 3/2) \delta_{n'_\rho}^{n_\rho} - \sqrt{n_\rho(n_\rho + l_\rho + 1/2)} \delta_{n'_\rho}^{n_\rho+1} - \sqrt{(n_\rho + 1)(n_\rho + l_\rho + 3/2)} \delta_{n'_\rho}^{n_\rho-1} \right], \\ &\langle n'_\rho l'_\rho m'_\rho n'_\lambda l'_\lambda m'_\lambda | \lambda^2 | n_\rho l_\rho m_\rho n_\lambda l_\lambda m_\lambda \rangle \\ &= \delta_{n'_\rho}^{n_\rho} \delta_{l'_\rho}^{l_\rho} \delta_{m'_\rho}^{m_\rho} \delta_{l'_\lambda}^{l_\lambda} \delta_{m'_\lambda}^{m_\lambda} \alpha^{-2} \left[(2n_\lambda + l_\lambda + 3/2) \delta_{n'_\lambda}^{n_\lambda} - \sqrt{n_\lambda(n_\lambda + l_\lambda + 1/2)} \delta_{n'_\lambda}^{n_\lambda+1} - \sqrt{(n_\lambda + 1)(n_\lambda + l_\lambda + 3/2)} \delta_{n'_\lambda}^{n_\lambda-1} \right]. \end{aligned} \quad (\text{D3})$$

Note that, the kinetic energy and root-mean-squared radius operators are diagonal in the spin and flavor spaces.

2. Azimuthal angles independent couplings

For the potential $\mathcal{V}_{ij}(\mathbf{r}_{ij})$ between quark i and quark j , the spin-independent terms and spin-spin coupling term depend only on the distance between two quarks, see Appendix A. For $\Phi(|\mathbf{r}_{12}|)$, we have simply

$$\langle n'_\rho l'_\rho m'_\rho n'_\lambda l'_\lambda m'_\lambda | \Phi(|\mathbf{r}_{12}|) | n_\rho l_\rho m_\rho n_\lambda l_\lambda m_\lambda \rangle = \delta_{l'_\rho}^{l_\rho} \delta_{m'_\rho}^{m_\rho} \delta_{n'_\lambda}^{n_\lambda} \delta_{l'_\lambda}^{l_\lambda} \delta_{m'_\lambda}^{m_\lambda} \int \rho^2 d\rho \psi_{n_\rho l_\rho}(\rho) \psi_{n'_\rho l'_\rho}(\rho) \Phi \left(\sqrt{\frac{m(\epsilon_1 + \epsilon_2)}{\epsilon_1 \epsilon_2}} \rho \right), \quad (\text{D4})$$

where $\psi_{nl}(r)$ is the radial sector of the spherical harmonic oscillator (11). Using the particle index rotation method defined in Appendix C, we obtain for $\Phi(|\mathbf{r}_{23}|)$ and $\Phi(|\mathbf{r}_{13}|)$,

$$\begin{aligned}
& \langle n'_\rho l'_\rho m'_\rho n'_\lambda l'_\lambda m'_\lambda | \Phi(|\mathbf{r}_{23}|) | n_\rho l_\rho m_\rho n_\lambda l_\lambda m_\lambda \rangle \\
&= \sum D_{n'_\rho l'_\rho m'_\rho n'_\lambda l'_\lambda m'_\lambda}^{\tilde{n}'_\rho \tilde{l}'_\rho \tilde{m}'_\rho \tilde{n}'_\lambda \tilde{l}'_\lambda \tilde{m}'_\lambda} [\theta_{23}] D_{n_\rho l_\rho m_\rho n_\lambda l_\lambda m_\lambda}^{\tilde{n}_\rho \tilde{l}_\rho \tilde{m}_\rho \tilde{n}_\lambda \tilde{l}_\lambda \tilde{m}_\lambda} [\theta_{23}] \int \tilde{\rho}^2 d\tilde{\rho} \psi_{\tilde{n}_\rho \tilde{l}_\rho}(\tilde{\rho}) \psi_{\tilde{n}'_\rho \tilde{l}'_\rho}(\tilde{\rho}) \Phi \left(\sqrt{\frac{\tilde{m}(\epsilon_2 + \epsilon_3)}{\epsilon_2 \epsilon_3}} \tilde{\rho} \right), \\
& \langle n'_\rho l'_\rho m'_\rho n'_\lambda l'_\lambda m'_\lambda | \Phi(|\mathbf{r}_{13}|) | n_\rho l_\rho m_\rho n_\lambda l_\lambda m_\lambda \rangle \\
&= \sum D_{n'_\rho l'_\rho m'_\rho n'_\lambda l'_\lambda m'_\lambda}^{\tilde{n}'_\rho \tilde{l}'_\rho \tilde{m}'_\rho \tilde{n}'_\lambda \tilde{l}'_\lambda \tilde{m}'_\lambda} [\theta_{13}] D_{n_\rho l_\rho m_\rho n_\lambda l_\lambda m_\lambda}^{\tilde{n}_\rho \tilde{l}_\rho \tilde{m}_\rho \tilde{n}_\lambda \tilde{l}_\lambda \tilde{m}_\lambda} [\theta_{13}] \int \tilde{\rho}^2 d\tilde{\rho} \psi_{\tilde{n}_\rho \tilde{l}_\rho}(\tilde{\rho}) \psi_{\tilde{n}'_\rho \tilde{l}'_\rho}(\tilde{\rho}) \Phi \left(\sqrt{\frac{\tilde{m}(\epsilon_1 + \epsilon_3)}{\epsilon_1 \epsilon_3}} \tilde{\rho} \right). \quad (\text{D5})
\end{aligned}$$

3. Azimuthal angles dependent couplings

The orbital angular momentum dependent terms and tensor term in $\mathcal{V}_{ij}(\mathbf{r}_{ij})$ depend on the azimuthal angles θ and ϕ of \mathbf{r}_{ij} . Note that, the couplings $\Phi_{SO}, \Phi_{SOT}, \Phi_{SOD}, \Phi_{SOX}$ and Φ_T shown in Appendix A depend only on the distance $|\hat{\mathbf{r}}_{ij}|$, the angle dependence comes from their coefficients $H(\boldsymbol{\sigma}_i, \boldsymbol{\sigma}_j, \mathbf{L}_{ij}, \hat{\mathbf{r}}_{ij})$ shown in (3). To calculate the elements of the coefficients in spin space, we first express the three-body spin states $|S\rangle$ shown in Appendix B as products of two-body spin state $|S, S_z\rangle_{ij}$ and single spin state $|s_z\rangle_k$,

$$\begin{aligned}
|S\rangle_{S1,2} &= |1, \pm 1\rangle_{12} |\pm 1/2\rangle_3 = |1, \pm 1\rangle_{23} |\pm 1/2\rangle_1 = |1, \pm 1\rangle_{31} |\pm 1/2\rangle_2, \\
|S\rangle_{S3,4} &= \sqrt{1/3} |1, \pm 1\rangle_{12} |\mp 1/2\rangle_3 + \sqrt{2/3} |1, 0\rangle_{12} |\pm 1/2\rangle_3 \\
&= \sqrt{1/3} |1, \pm 1\rangle_{23} |\mp 1/2\rangle_1 + \sqrt{2/3} |1, 0\rangle_{23} |\pm 1/2\rangle_1 \\
&= \sqrt{1/3} |1, \pm 1\rangle_{13} |\mp 1/2\rangle_2 + \sqrt{2/3} |1, 0\rangle_{13} |\pm 1/2\rangle_2, \\
|S\rangle_{MS1,2} &= \sqrt{2/3} |1, \pm 1\rangle_{12} |\mp 1/2\rangle_3 - \sqrt{1/3} |1, 0\rangle_{12} |\pm 1/2\rangle_3 \\
&= \sqrt{3/4} |0, 0\rangle_{23} |\pm 1/2\rangle_1 - \sqrt{1/12} |1, 0\rangle_{23} |\pm 1/2\rangle_1 + \sqrt{1/6} |1, \pm 1\rangle_{23} |\mp 1/2\rangle_1 \\
&= -\sqrt{3/4} |0, 0\rangle_{13} |\pm 1/2\rangle_2 - \sqrt{1/12} |1, 0\rangle_{13} |\pm 1/2\rangle_2 + \sqrt{1/6} |1, \pm 1\rangle_{13} |\mp 1/2\rangle_2, \\
|S\rangle_{MA1,2} &= |0, 0\rangle_{12} |\pm 1/2\rangle_3 \\
&= -1/2 |0, 0\rangle_{23} |\pm 1/2\rangle_1 + 1/2 |1, 0\rangle_{23} |\pm 1/2\rangle_1 - \sqrt{1/2} |1, \pm 1\rangle_{23} |\mp 1/2\rangle_1 \\
&= -1/2 |0, 0\rangle_{13} |\pm 1/2\rangle_2 - 1/2 |1, 0\rangle_{13} |\pm 1/2\rangle_2 + \sqrt{1/2} |1, \pm 1\rangle_{13} |\mp 1/2\rangle_2, \quad (\text{D6})
\end{aligned}$$

where one can clearly see that, the mixed antisymmetric states correspond to the spin singlet of the first two quarks, and the symmetric and mixed symmetric states correspond to all the triplets.

Employing the algebraic method used in quantum mechanics, we introduce the ladder operators for the single spin operator \mathbf{s}_i , orbital angular momentum \mathbf{L}_{ij} and relative coordinate $\hat{\mathbf{r}}_{ij}$, $s^\pm = (s_x \pm i s_y)/\sqrt{2}$, $L^\pm = (L_x \pm i L_y)/\sqrt{2}$ and $\hat{r}^\pm = (\hat{r}_x \pm i \hat{r}_y)/\sqrt{2} = \sin \theta e^{\pm i \phi}/\sqrt{2}$, and express the spin dependent coefficients H in terms of the ladder operators,

$$\begin{aligned}
\mathbf{L} \cdot \mathbf{s} &= L_z s_z + L^+ s^- + L^- s^+, \\
\mathbf{s}_i \cdot \mathbf{s}_j &= s_{iz} s_{jz} + s_i^+ s_j^- + s_i^- s_j^+, \\
\hat{\mathbf{r}} \cdot \mathbf{s} &= \hat{r}_z s_z + \hat{r}^+ s^- + \hat{r}^- s^+ \quad (\text{D7})
\end{aligned}$$

which lead to the following raising and lowering relations for the orbital angular momentum state and single spin

state,

$$\begin{aligned}
L_z |l, m\rangle &= m |l, m\rangle, \\
L^\pm |l, m\rangle &= \sqrt{(l \pm m + 1)(l \mp m)/2} |l, m \pm 1\rangle, \\
\hat{r}_z |l, m\rangle &= \sqrt{\frac{(l + l' + 1)^2 - 4m^2}{4(2l + 1)(2l' + 1)}} (\delta_{l'}^{l+1} + \delta_{l'}^{l-1}) |l', m\rangle, \\
\hat{r}^\pm |l, m\rangle &= \mp \left[\sqrt{\frac{(l + 1 \pm m)(l' + 1 \pm m)}{2(2l + 1)(2l' + 1)}} \delta_{l'}^{l+1} - \sqrt{\frac{(l \mp m)(l' \mp m)}{2(2l + 1)(2l' + 1)}} \delta_{l'}^{l-1} \right] |l', m \pm 1\rangle, \\
s_z |\pm 1/2\rangle &= \pm 1/2 |\pm 1/2\rangle, \\
s^+ |1/2\rangle &= 0, \quad s^+ |-1/2\rangle = \sqrt{1/2} |1/2\rangle, \quad s^- |1/2\rangle = \sqrt{1/2} |-1/2\rangle, \quad s^- |-1/2\rangle = 0.
\end{aligned} \tag{D8}$$

With the above preparation we are now ready to compute the matrix elements of the coupling terms $H(\boldsymbol{\sigma}_i, \boldsymbol{\sigma}_j, \mathbf{L}_{ij}, \hat{\mathbf{r}}_{ij})\Phi(|\mathbf{r}_{ij}|)$. For a given flavor state $|q_i q_j q_k\rangle$ shown in Appendix B, a given spin state $|S, S_z\rangle |s_z\rangle$ shown above, and a given spherical harmonic oscillator $|n_\rho l_\rho m_\rho n_\lambda l_\lambda m_\lambda\rangle$ with $\mathbf{r}_{ij} \sim \boldsymbol{\rho}$ (if not, making particle index rotation before), we have

$$\begin{aligned}
&\langle n'_\rho l'_\rho m'_\rho n'_\lambda l'_\lambda m'_\lambda | \langle S', S'_z | \langle s_z | H(\boldsymbol{\sigma}_i, \boldsymbol{\sigma}_j, \mathbf{L}_{ij}, \hat{\mathbf{r}}_{ij}) \Phi(|\mathbf{r}_{ij}|) | S, S_z \rangle | s_z \rangle | n_\rho l_\rho m_\rho n_\lambda l_\lambda m_\lambda \rangle \\
&= \delta_{n'_\lambda}^{n_\lambda} \delta_{l'_\lambda}^{l_\lambda} \delta_{m'_\lambda}^{m_\lambda} \delta_{s'_z}^{s_z} \langle l'_\rho m'_\rho | \langle S', S'_z | H(\boldsymbol{\sigma}_i, \boldsymbol{\sigma}_j, \mathbf{L}_{ij}, \hat{\mathbf{r}}_{ij}) | S, S_z \rangle | l_\rho m_\rho \rangle \int \psi_{n_\rho l_\rho}(\rho) \psi_{n'_\rho l'_\rho}(\rho) \Phi\left(\sqrt{\frac{\overline{m}(\epsilon_i + \epsilon_j)}{\epsilon_i \epsilon_j}} \rho\right) \rho^2 d\rho.
\end{aligned} \tag{D9}$$

The elements $H_{LS, L'S'} = \langle l'_\rho m'_\rho | \langle S', S'_z | H(\boldsymbol{\sigma}_i, \boldsymbol{\sigma}_j, \mathbf{L}_{ij}, \hat{\mathbf{r}}_{ij}) | S, S_z \rangle | l_\rho m_\rho \rangle$ in angular momentum space can be analytically calculated. It is direct to obtain

$$H_{LS, L'S'}^{SS} = [2S(S + 1) - 3] \delta_{l'_\rho}^{l_\rho} \delta_{m'_\rho}^{m_\rho} \delta_{S'}^{S} \delta_{S'_z}^{S_z} \tag{D10}$$

for spin-spin coupling with $H = \boldsymbol{\sigma}_i \cdot \boldsymbol{\sigma}_j$,

$$H_{LS, L'S'}^{SO} = \left[2m_\rho S_z \delta_{m'_\rho}^{m_\rho} \delta_{S'_z}^{S_z} + D_{l'_\rho}^{m_\rho} D_{S'_z}^{S_z} \delta_{m'_\rho+1}^{m_\rho} \delta_{S'_z-1}^{S_z} + D_{l'_\rho}^{m'_\rho} D_{S'_z}^{S'_z} \delta_{m'_\rho-1}^{m_\rho} \delta_{S'_z+1}^{S_z} \right] \delta_{l'_\rho}^{l_\rho} \delta_{S'}^{S} \tag{D11}$$

with $D_l^m = \sqrt{(l + m + 1)(l - m)}$ for spin-orbital coupling with $H = \mathbf{L}_{ij} \cdot (\boldsymbol{\sigma}_i + \boldsymbol{\sigma}_j)$,

$$\begin{aligned}
H_{LS, L'S'}^{SOD} &= \left[2m_\rho \left((1 - S) \delta_{S+1}^{S'_z} + (S^2 - S_z^2) \delta_{S-1}^{S'_z} \right) \delta_{m'_\rho}^{m_\rho} \delta_{S'_z}^{S_z} \right. \\
&\quad + \sqrt{(S - S_z - 1)(S - S_z - 2)} D_{l'_\rho}^{m_\rho} \left((1 - S) \delta_{S+1}^{S'_z} - S \delta_{S-1}^{S'_z} \right) \delta_{m'_\rho+1}^{m_\rho} \delta_{S'_z-1}^{S_z} \\
&\quad \left. - \sqrt{(S + S_z - 1)(S + S_z - 2)} D_{l'_\rho}^{m'_\rho} \left((1 - S) \delta_{S+1}^{S'_z} - S \delta_{S-1}^{S'_z} \right) \delta_{m'_\rho-1}^{m_\rho} \delta_{S'_z+1}^{S_z} \right] \delta_{l'_\rho}^{l_\rho}
\end{aligned} \tag{D12}$$

for spin-orbital difference coupling with $H = \mathbf{L}_{ij} \cdot (\boldsymbol{\sigma}_i - \boldsymbol{\sigma}_j)$,

$$\begin{aligned}
H_{LS, L'S'}^{SOX} &= \left[2m_\rho \left((1 - S) \delta_{S+1}^{S'_z} - (S^2 - S_z^2) \delta_{S-1}^{S'_z} \right) \delta_{m'_\rho}^{m_\rho} \delta_{S'_z}^{S_z} \right. \\
&\quad + \sqrt{(S - S_z - 1)(S - S_z - 2)} D_{l'_\rho}^{m_\rho} \left((1 - S) \delta_{S+1}^{S'_z} + S \delta_{S-1}^{S'_z} \right) \delta_{m'_\rho+1}^{m_\rho} \delta_{S'_z-1}^{S_z} \\
&\quad \left. - \sqrt{(S + S_z - 1)(S + S_z - 2)} D_{l'_\rho}^{m'_\rho} \left((1 - S) \delta_{S+1}^{S'_z} + S \delta_{S-1}^{S'_z} \right) \delta_{m'_\rho-1}^{m_\rho} \delta_{S'_z+1}^{S_z} \right] \delta_{l'_\rho}^{l_\rho}
\end{aligned} \tag{D13}$$

for spin-orbital cross coupling with $H = i\mathbf{L}_{ij} \cdot (\boldsymbol{\sigma}_i \times \boldsymbol{\sigma}_j)$,

$$\begin{aligned}
& H_{LS,L'S'}^T \\
&= [6S_z^2 - 2S(S+1)] \left[\frac{l_\rho^2 + l_\rho - 3m_\rho^2}{4l_\rho^2 + 4l_\rho - 3} \delta_{l_\rho}^{l'_\rho} + \frac{3}{2} \sqrt{\frac{((l_\rho + l'_\rho)^2 - 4m_\rho^2)((l_\rho + l'_\rho + 2)^2 - 4m_\rho^2)}{16(2l_\rho + 1)(2l'_\rho + 1)(l_\rho + l'_\rho + 1)^2}} (\delta_{l_\rho+2}^{l'_\rho} + \delta_{l_\rho-2}^{l'_\rho}) \right] \delta_S^{S'} \delta_{S_z}^{S'_z} \delta_{m_\rho}^{m'_\rho} \\
&\quad - \sqrt{1/2}(S + S_z)(2S - 3S_z) \left[\sqrt{\frac{(l_\rho - m_\rho + 1)\Gamma(l_\rho + m_\rho + 4)/\Gamma(l_\rho + m_\rho + 1)}{(2l_\rho + 1)(2l'_\rho + 1)(l_\rho + l'_\rho + 1)^2}} \delta_{l_\rho+2}^{l'_\rho} \right. \\
&\quad \left. - \sqrt{\frac{(l_\rho + m_\rho)\Gamma(l_\rho - m_\rho + 1)/\Gamma(l_\rho - m_\rho - 2)}{(2l_\rho + 1)(2l'_\rho + 1)(l_\rho + l'_\rho + 1)^2}} \delta_{l_\rho-2}^{l'_\rho} + \frac{(m_\rho + m'_\rho)\sqrt{(l_\rho + m_\rho + 1)(l_\rho - m_\rho)}}{4l_\rho^2 + 4l_\rho - 3} \delta_{l_\rho}^{l'_\rho} \right] \delta_S^{S'} \delta_{S_z-1}^{S'_z} \delta_{m_\rho+1}^{m'_\rho} \\
&\quad - \sqrt{1/2}(S - S_z)(2S + 3S_z) \left[+ \sqrt{\frac{(l_\rho + m_\rho + 1)\Gamma(l_\rho - m_\rho + 4)/\Gamma(l_\rho - m_\rho + 1)}{(2l_\rho + 1)(2l'_\rho + 1)(l_\rho + l'_\rho + 1)^2}} \delta_{l_\rho+2}^{l'_\rho} \right. \\
&\quad \left. - \sqrt{\frac{(l_\rho - m_\rho)\Gamma(l_\rho + m_\rho + 1)/\Gamma(l_\rho + m_\rho - 2)}{(2l_\rho + 1)(2l'_\rho + 1)(l_\rho + l'_\rho + 1)^2}} \delta_{l_\rho-2}^{l'_\rho} - \frac{(m_\rho + m'_\rho)\sqrt{(l_\rho - m_\rho + 1)(l_\rho + m_\rho)}}{4l_\rho^2 + 4l_\rho - 3} \delta_{l_\rho}^{l'_\rho} \right] \delta_S^{S'} \delta_{S_z+1}^{S'_z} \delta_{m_\rho-1}^{m'_\rho} \\
&\quad - \sqrt{2}(S + S_z)(S + S_z - 1) \left[\sqrt{\frac{((l_\rho + 1)^2 - (m_\rho + 1)^2)(l_\rho^2 - (m_\rho + 1)^2)}{4l_\rho^2 + 4l_\rho - 3}} \delta_{l_\rho}^{l'_\rho} \right. \\
&\quad \left. - \sqrt{\frac{\Gamma(l_\rho + m_\rho + 5)/\Gamma(l_\rho + m_\rho + 1)}{4(2l_\rho + 1)(2l'_\rho + 1)(l_\rho + l'_\rho + 1)^2}} \delta_{l_\rho+2}^{l'_\rho} - \sqrt{\frac{\Gamma(l_\rho - m_\rho + 1)/\Gamma(l_\rho - m_\rho - 3)}{4(2l_\rho + 1)(2l'_\rho + 1)(l_\rho + l'_\rho + 1)^2}} \delta_{l_\rho-2}^{l'_\rho} \right] \delta_S^{S'} \delta_{S_z-2}^{S'_z} \delta_{m_\rho+2}^{m'_\rho} \\
&\quad - \sqrt{2}(S - S_z)(S - S_z - 1) \left[\sqrt{\frac{((l_\rho + 1)^2 - (m_\rho - 1)^2)(l_\rho^2 - (m_\rho - 1)^2)}{4l_\rho^2 + 4l_\rho - 3}} \delta_{l_\rho}^{l'_\rho} \right. \\
&\quad \left. - \sqrt{\frac{\Gamma(l_\rho - m_\rho + 5)/\Gamma(l_\rho - m_\rho + 1)}{4(2l_\rho + 1)(2l'_\rho + 1)(l_\rho + l'_\rho + 1)^2}} \delta_{l_\rho+2}^{l'_\rho} - \sqrt{\frac{\Gamma(l_\rho + m_\rho + 1)/\Gamma(l_\rho + m_\rho - 3)}{4(2l_\rho + 1)(2l'_\rho + 1)(l_\rho + l'_\rho + 1)^2}} \delta_{l_\rho-2}^{l'_\rho} \right] \delta_S^{S'} \delta_{S_z+2}^{S'_z} \delta_{m_\rho-2}^{m'_\rho} \quad (D14)
\end{aligned}$$

for tensor coupling with $H = 3(\boldsymbol{\sigma}_i \cdot \hat{\mathbf{r}}_{ij})(\boldsymbol{\sigma}_j \cdot \hat{\mathbf{r}}_{ij}) - \boldsymbol{\sigma}_i \cdot \boldsymbol{\sigma}_j$, and

$$H_{LS,L'S'}^{SOT} = \frac{1}{3} \sum \left(H_{L'S',L''S''}^T + H_{L'S',L''S''}^{SS} \right) H_{L''S'',LS}^{SO} \quad (D15)$$

for spin-orbital tensor coupling with $H = (\boldsymbol{\sigma}_i \cdot \hat{\mathbf{r}}_{ij})(\boldsymbol{\sigma}_j \cdot \hat{\mathbf{r}}_{ij})(\mathbf{L}_{ij} \cdot (\boldsymbol{\sigma}_i + \boldsymbol{\sigma}_j))$.

-
- [1] R. Aaij *et al.* [LHCb Collaboration], Phys. Rev. Lett. **119**, no. 11, 112001 (2017).
[2] R. Aaij *et al.* [LHCb Collaboration], Phys. Rev. Lett. **115**, 072001 (2015).
[3] M. Fukugita, Y. Oyanagi and A. Ukawa, Phys. Rev. Lett. **57**, 953 (1986).
[4] F. Butler, H. Chen, J. Sexton, A. Vaccarino and D. Weingarten, Nucl. Phys. B **430**, 179 (1994).
[5] A. Ali Khan *et al.* [CP-PACS Collaboration], Phys. Rev. D **65**, 054505 (2002) Erratum: [Phys. Rev. D **67**, 059901 (2003)].
[6] Y. Namekawa *et al.* [PACS-CS Collaboration], Phys. Rev. D **87**, no. 9, 094512 (2013).
[7] Z. S. Brown, W. Detmold, S. Meinel and K. Orginos, Phys. Rev. D **90**, no. 9, 094507 (2014).
[8] Z. G. Wang, Phys. Lett. B **685**, 59 (2010).
[9] P. Maris and P. C. Tandy, Phys. Rev. C **60**, 055214 (1999).
[10] M. K. Volkov, D. Ebert and M. Nagy, Int. J. Mod. Phys. A **13**, 5443 (1998).
[11] H. Satz, J. Phys. G **32**, R25 (2006).
[12] H. He, Y. Liu and P. Zhuang, Phys. Lett. B **746**, 59 (2015).
[13] J. Zhao, H. He and P. Zhuang, Phys. Lett. B **771**, 349 (2017).
[14] J. Zhao and P. Zhuang, Few Body Syst. **58**, no. 2, 100 (2017).
[15] N. Isgur and G. Karl, Phys. Rev. D **20**, 1191 (1979).
[16] N. Isgur and G. Karl, Phys. Rev. D **19**, 2653 (1979).
[17] E. E. Salpeter and H. A. Bethe, Phys. Rev. **84**, 1232 (1951).
[18] M. Gell-Mann and F. Low, Phys. Rev. **84**, 350 (1951).
[19] A. A. Logunov and A. N. Tavkhelidze, Nuovo Cim. **29**, 380 (1963).

- [20] F. Gross, Phys. Rev. **186**, 1448 (1969).
- [21] H. Sazdjian, J. Math. Phys. **28**, 2618 (1987).
- [22] H. W. Crater and P. Van Alstine, Annals Phys. **148**, 57 (1983).
- [23] H. W. Crater and P. Van Alstine, Phys. Rev. D **36**, 3007 (1987).
- [24] H. W. Crater, J. H. Yoon and C. Y. Wong, Phys. Rev. D **79**, 034011 (2009).
- [25] J. F. Whitney and H. W. Crater, Phys. Rev. D **89**, no. 1, 014023 (2014).
- [26] X. Guo, S. Shi and P. Zhuang, Phys. Lett. B **718**, 143 (2012).
- [27] S. Shi, X. Guo and P. Zhuang, Phys. Rev. D **88**, no. 1, 014021 (2013).
- [28] E. Eichten, K. Gottfried, T. Kinoshita, K. D. Lane and T. M. Yan, Phys. Rev. D **17**, 3090 (1978) Erratum: [Phys. Rev. D **21**, 313 (1980)].
- [29] M. D. Schwartz, “Quantum Field Theory and the Standard Model,” Cambridge University Press (2014). pp 513.
- [30] C. Alexandrou, P. de Forcrand and O. Jahn, Nucl. Phys. Proc. Suppl. **119**, 667 (2003).
- [31] Krivec, R., Few-Body Systems, **25**, 199 (1998).
- [32] R. Krivec and M. V. Mihailovic, Phys. Lett. B **181**, 1 (1986).
- [33] E. Hiyama and M. Kamimura, Front. Phys. (Beijing) **13**, no. 6, 132106 (2018).
- [34] S. Capstick and N. Isgur, Phys. Rev. D **34**, 2809 (1986).
- [35] M. Tanabashi *et al.* [Particle Data Group], Phys. Rev. D **98**, no. 3, 030001 (2018).
- [36] B. Silvestre-Brac, Few Body Syst. **20**, 1 (1996).
- [37] R. J. Fries, B. Muller, C. Nonaka and S. A. Bass, Phys. Rev. C **68**, 044902 (2003).
- [38] V. Greco, C. M. Ko and P. Levai, Phys. Rev. C **68**, 034904 (2003).
- [39] S. Digal, O. Kaczmarek, F. Karsch and H. Satz, Eur. Phys. J. C **43**, 71 (2005).
- [40] O. Kaczmarek, Eur. Phys. J. C **61**, 811 (2009).
- [41] J. Zhao and P. Zhuang, Phys. Lett. B **775**, 84 (2017).